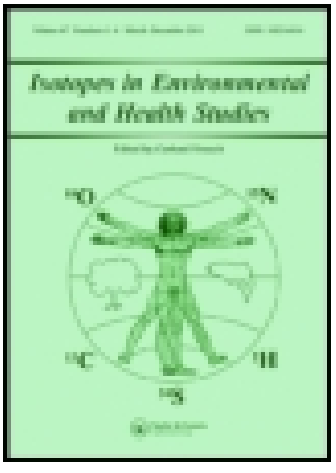

Isotopes in Environmental and Health Studies

Publication details, including instructions for authors and subscription information:
http://www.tandfonline.com/loi/gieh20

A study of the characteristics of karst groundwater circulation based on multi-isotope approach in the Liulin spring area, North China

Hongfei Zang[a], Xiuqing Zheng[a], Zuodong Qin[b] & Zhenxing Jia[ac]

[a] College of Water Resources Science and Engineering, Taiyuan University of Technology, Taiyuan, People's Republic of China

[b] Institute of Loess Plateau, Shanxi University, Taiyuan, People's Republic of China

[c] Shanxi Institute of Water Resources, Taiyuan, People's Republic of China

Published online: 15 Dec 2014.

To cite this article: Hongfei Zang, Xiuqing Zheng, Zuodong Qin & Zhenxing Jia (2014): A study of the characteristics of karst groundwater circulation based on multi-isotope approach in the Liulin spring area, North China, Isotopes in Environmental and Health Studies, DOI: 10.1080/10256016.2015.987275

To link to this article: http://dx.doi.org/10.1080/10256016.2015.987275

Isotopes in Environmental and Health Studies, 2014
http://dx.doi.org/10.1080/10256016.2015.987275

Taylor & Francis
Taylor & Francis Group

A study of the characteristics of karst groundwater circulation based on multi-isotope approach in the Liulin spring area, North China

Hongfei Zang[a], Xiuqing Zheng[a*], Zuodong Qin[b] and Zhenxing Jia[a,c]

[a]*College of Water Resources Science and Engineering, Taiyuan University of Technology, Taiyuan, People's Republic of China;* [b]*Institute of Loess Plateau, Shanxi University, Taiyuan, People's Republic of China;* [c]*Shanxi Institute of Water Resources, Taiyuan, People's Republic of China*

(*Received 12 April 2014; accepted 19 September 2014*)

Due to the significance of karst groundwater for water supply in arid and semi-arid regions, the characteristics of the karst groundwater flow system in the Liulin spring area, North China, are analysed through isotopic tracing (δ^2H, δ^{18}O, δ^{13}C and ^{3}H) and dating approaches (^{14}C). The results show that the primary recharge source of karst groundwater is precipitation. Evaporation during dropping and infiltration of rainfall results in a certain offset in the values of δ^2H and δ^{18}O in groundwater samples from the global meteoric water line (GMWL) and the local meteoric water line (LMWL). The altitudes of the recharge region calculated by δ^{18}O range from 1280 to 2020 m above sea level, which is consistent with the altitudes of the recharge area. The Liulin spring groups could be regarded as the mixing of groundwater with long and short flow paths at a ratio of 4:1. In the upgradient of the Liulin spring, the groundwater represents modern groundwater features and its HCO_3^- is mainly derived from dissolution of soil CO_2, while in the downgradient of the Liulin spring, the ^{14}C age of dissolved inorganic carbon (DIC) in groundwater shows an apparent increase and HCO_3^- is mainly derived from the dissolution of carbonate rocks. The mean flow rate calculated by ^{14}C ages of DIC between IS10 and IS12 is 1.23 m/year.

Keywords: age dating; carbon-13; carbon-14; hydrogen-2; hydrogen-3; hydrogeochemistry; isotope geology; karst groundwater; Liulin spring area; oxygen-18; water supply

1. Introduction

Water resource shortages are the primary constraint for the local economic development and the improvement of living conditions for the residents in the Liulin spring area. Due to the lack of an adequate surface water supply, karst groundwater is the major water supply source in this area. Thus, research on the groundwater flow system that controls water quantity and quality is crucial.

Environmental isotope methods are used as the most conclusive tool available to deal with the complicated hydrogeological problems in the karst region [1–5]. Deuterium (^{2}H), tritium (^{3}H), oxygen-18 (^{18}O), carbon-13 (^{13}C) and carbon-14 (^{14}C) are the most frequently used environmental isotopes. As they are not influenced by water–rock interactions at room temperature, ^{2}H and ^{18}O are usually used to determine the recharge source and residence time of groundwater, as well as the altitude and location of recharge regions [4–15]. Generally, ^{13}C is used for analysing

*Corresponding author. Email: zhengxiuqing@tyut.edu.cn

biogeochemical processes and DIC cycles in the groundwater [16–22]. The radioactive isotopes ^{3}H and ^{14}C, which are formed in the lower stratosphere/upper troposphere under natural conditions and have spontaneous radioactive decay, are used to explore runoff conditions and calculate the residence time of the groundwater flow [12,23].

Previous research on isotopic features of the groundwater flow system in the Liulin spring area is limited. Yang et al. [24] established the meteoric water line of the Ordos basin and studied the isotopic features of shallow groundwater. By means of isotopic methods, Lin and Wang [25] divided the karst groundwater system of the Liulin spring area into two subsystems, the shallow subsystem and the deep subsystem; Ma et al. [26] explored the source of thermal karst groundwater in the Taiyuan basin near the Liulin spring area. More often, isotopic methods were used to supplement and verify the conventional hydrogeochemical data. Systematic study of the isotopic features is important in an area with complex hydrogeological condition and lower degree of research, such as the Liulin spring area.

The characteristics of karst groundwater flow system of the Liulin spring area are analysed by using environmental isotope tracing and dating methods. The recharge source and mean altitude of recharge regions of groundwater are determined by $\delta^{2}H$ and $\delta^{18}O$; the mixing and runoff features of the karst groundwater are analysed by ^{3}H and the residence time and DIC cycles are determined by ^{14}C and $\delta^{13}C$.

2. Liulin spring area

2.1. *Physical geography*

The Liulin spring area, which covers 6080.54 km^2, lies between the western Shanxi Loess Plateau and the Lvliang Ranges. The study area is subject to continental monsoon climate with a mean annual temperature of 9.2 °C, mean relative air humidity of 54 ∼ 62%, rainfall of 508 mm and evaporation of 1186 mm [27]. The rainfall in July, August and September takes up approximately 66 % of the annual precipitation. The Sanchuan river and its tributaries, including the Beichuan river, the Dongchuan river and the Nanchuan river, are the major surface water sources (Figure 1). The surface elevation ranges from 800 m above sea level (asl) in the West to 2800 m asl in the East. The Liulin spring, consisting of Zhaidong springs group, Shangqinglong springs group, Longmenhui springs group, Yangjiagang springs group and Liujiageda springs group, occurs in the valley of the Sanchuan river between Zhaidong village and Shangqinglong village in Liulin County (Figure 1). Their elevations vary from ∼792 to 803 m asl, and the total mean annual discharge is 2.37 m^3/s.

2.2. *Geology and hydrogeology*

Precambrian metamorphic rock outcroppings can be found in the northern, eastern and southern regions, while Cambrian–Ordovician carbonate strata outcrop mostly in the south-eastern and central regions (Figure 1). Carboniferous–Triassic clastic rocks mainly distribute in the west and central regions. Tertiary and Quaternary deposits overlie various ages of the bedrock. From a geotectonic point of view, the spring area belongs to the east limb of the Ordos syncline basin with a 2–8°dip angle, within which secondary folds and fractures develop (Figure 2). The geologic structure dominates the directions of the groundwater flow.

The northern and eastern boundaries of spring area are composed of drainage divides in metamorphic rock mountains, whereas the southern and south-eastern boundaries consist of subsurface divides in the exposed areas of carbonate rocks. In the west, carbonate rocks inclined

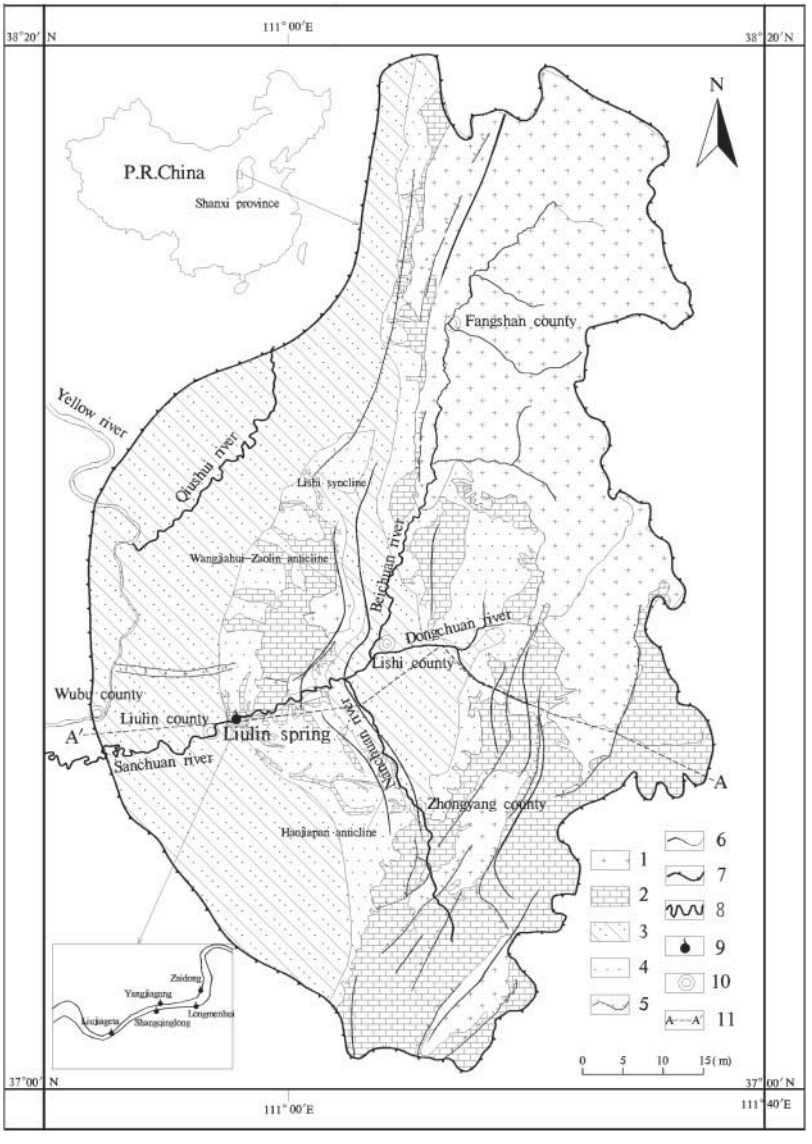

Figure 1. Simplified geological map of the Liulin karst water system with an enlarged view of the locations of springs. 1. Precambrian metamorphic rocks; 2. Cambrian and Ordovician carbonate rocks; 3. Carboniferous–Triassic clastic rocks; 4. Neogene–Quaternary rickle; 5. fault; 6. fold; 7. boundary of spring area; 8. river; 9. spring; 10. city; 11. cross hatching A–A′.

towards the syncline core of the Ordos Basin are overlaid by hundreds of metres of thick-bedded clastic rocks (Figure 2) where karst groundwater has no discharge path [27]. Hence the karst groundwater is stagnant in this region. This boundary was defined as the lines where the burial depth of Ordovician carbonate rocks reaches to 1000 m. Cambrian and Ordovician marine carbonate rocks constitute the main aquifer, in which the middle series of the Ordovician rocks consisting of limestone, dolomite and some gypsum is the main source for water supply.

The karst groundwater system is mainly recharged by precipitation in exposed areas of carbonate rocks (Figure 2), next to the leakage of river water from the Shanchuan river. In the centre of the spring area, carbonate rocks are covered by a thick interbed of sandstone and

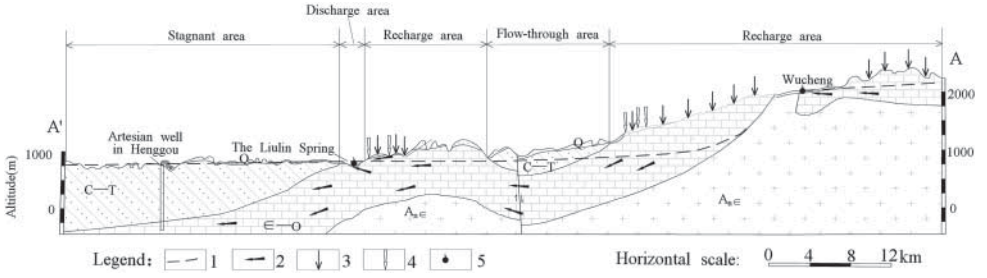

Figure 2. Hydrogeological cross section of the Liulin spring area. The cross hatching A–A′ is shown in Figure 1. 1. Karst groundwater table; 2. flow directions of groundwater; 3. recharge of precipitation; 4. recharge of surface water; 5. spring.

mudstone, which prevent the precipitation from recharging the aquifer, and this region is defined as the flow-through area. Karst groundwater flows from the North, East and South towards the Liulin spring. Spring discharge in the Sanchuan river valley and well exploitation are two major discharge ways in the groundwater system.

3. Sampling and analysis

Ten karst groundwater samples were collected from the wells and springs in Ordovician carbonate rocks aquifer along the main groundwater flow path (Figure 3) in May 2011. The values of δ^2H, δ^{18}O, ^{3}H, δ^{13}C and ^{14}C were analysed for each sample at the Institute of Hydrogeology and Environmental Geology, Chinese Academy of Geological Sciences. Furthermore, three groups of isotopic data sampled by the Geological Survey Institute of Shanxi Province in June 2002 were used for supplementary and comparative purposes [28]. The isotopic measurement results and details of the sampling sites are presented in Table 1.

Water temperature and pH values were measured *in situ*. The concentration of HCO_3^- was measured on the sampling day via the Gran titration method [29]. The isotopic composition of oxygen (δ^{18}O) was measured using a MAT253 mass spectrometer with a precision of $\sigma \leq 0.1‰$ after equilibration with reference CO_2 at 25 °C for 24 h. The measurement of δ^2H was performed on a MAT253 mass spectrometer via the chromium reduction method with a precision of $\sigma \leq 2‰$. Using the phosphoric acid method, δ^{13}C of the DIC was measured by the MAT253 mass spectrometer with a precision of $\sigma \leq 0.1‰$. Tritium (^{3}H) and radioactive carbon (^{14}C) contents were determined by the electrolytic enrichment method and the benzene synthesis method, respectively. Both of them were measured via an ultra-low-background liquid scintillation spectrometer (1220 Quantulus) with a detection limit of 0.6 TU for ^{3}H and 0.2 % pMC (percentage of modern carbon) for ^{14}C.

The measurements of δ^2H, δ^{18}O and δ^{13}C were reported in the standard δ-notation in per mille (‰) [30,31]:

$$\delta = \frac{R - R_S}{R_S}, \tag{1}$$

where R is the heavy-to-light isotope ratio (e.g. ^{18}O/^{16}O) of the sample and R_S is the isotope ratio of the reference material. δ^2H and δ^{18}O are reported relative to the Vienna standard mean ocean water, while ^{13}C is reported relative to the Vienna Pee Dee Belemnite. ^{3}H is denoted by tritium units (TU) and ^{14}C is given in pMC.

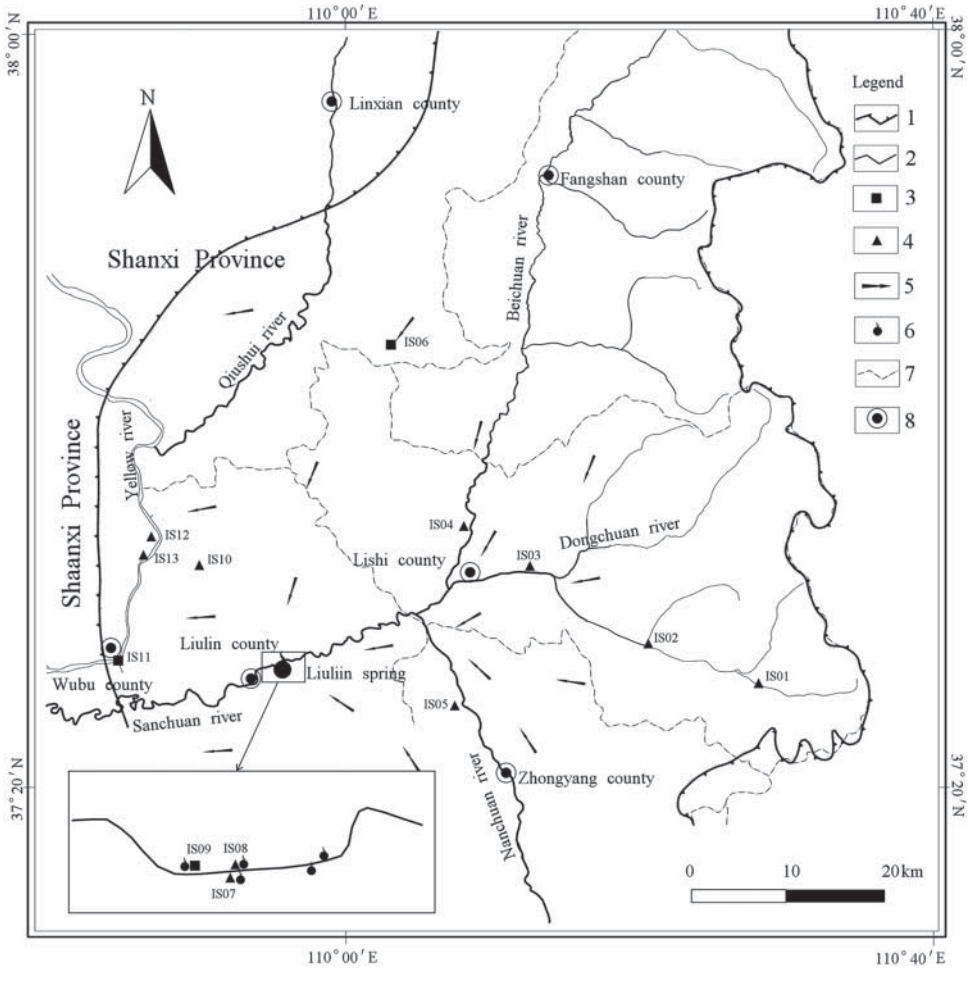

Figure 3. Map of study area showing the sampling sites. 1. Boundary of spring area; 2. river system; 3. sampling sites in June 2002; 4. sampling sites in May 2011; 5. flow directions of karst groundwater; 6. springs; 7. county boundary; 8. city.

4. Results and discussion

4.1. *Recharge source and altitude of the karst groundwater system*

4.1.1. *Recharge source*

For lack of isotopic composition data of precipitation in the study area, 20 groups of $\delta^{18}O$ and $\delta^{2}H$ values measured at Taiyuan Station (37.78 ° N, 112.55 ° E, 778 m asl) in the Global Network of Isotopes in Precipitation between 1986 and 1988 are used to fit the LMWL [32]. This station is 130 km away from Lishi County and its climate is similar to that of the study area. The weighted annual mean values for $\delta^{18}O$ and $\delta^{2}H$ are -7.24 and -51.2‰, respectively. The weighted mean value of d-excess ($d = \delta^{2}H - 8 \times \delta^{18}O$) is 6.78‰, lower than that of the GMWL ($d = 10$ ‰) [33,34], indicating that the humidity of the vapour source region is higher than the global mean value. The established LMWL is

$$\delta^{2}H = 6.42(\pm 0.36) \times \delta^{18}O - 4.66(\pm 2.95)(n = 20, R^{2} = 0.945) \quad (2)$$

Table 1. Isotopic composition of karst groundwater in the Liulin spring area.

No.	Area	Sampling time	Location	Type	Altitude (m)	Temperature (°C)	pH	TDS[a] (mg/L)	δ^2H (‰)	δ^{18}O (‰)	^{3}H (TU)	δ^{13}C (‰)	d-excess[b]	Recharge altitude[c] (m)
IS01	Recharge area	May 2011	Wucheng	Well	1339	11	7.7	280	− 72	− 10.5	26.7 ± 1.9	− 9.3	12.0	1830
IS02	Recharge area	May 2011	Youfangping	Well	1203	12	7.8	320	− 70	− 9.9	20.8 ± 1.6	− 10.4	9.2	1640
IS03	Flow-through area	May 2011	Tianjiahui	Well	988	17	7.9	330	− 71	− 9.9	11.3 ± 1.5	− 9.6	8.2	1640
IS04	Flow-through area	May 2011	Shang'an	Well	962	12	7.6	396	− 72	− 10.0	3.6 ± 1.2	− 10.9	8.0	1670
IS05	Flow-through area	May 2011	Jinluo	Well	960	15	7.5	416	− 73	− 9.5	3.8 ± 1.3	− 10.0	3.0	1510
IS06	Flow-through area	June 2002	Xize	Well	1055	21	7.7	/	− 70	− 9.5	15.4 ± 2.6	− 9.6	6.0	1510
IS07	Discharge area	May 2011	Shangqinglong	Spring	800	16	7.6	402	− 70	− 9.3	7.1 ± 1.4	− 9.6	4.4	1440
IS08	Discharge area	May 2011	Yangjiagang	Spring	808	13	7.6	970	− 69	− 8.8	9.0 ± 1.4	− 9.9	1.4	1280
IS09	Discharge area	June 2002	Liujiageta	Spring	801	20	7.5	/	− 69	− 9.8	8.5 ± 2.5	− 9.0	9.4	1600
IS10	Stagnant area	May 2011	Baijiayan	Well	849	23	7.2	1780	− 74	− 9.7	1.8 ± 1.2	− 9.0	3.6	1570
IS11	Stagnant area	June 2002	Wubu	Well	636	18	7.1	/	− 71	− 10.7	2.0 ± 2.32	− 5.4	14.6	1890
IS12	Stagnant area	May 2011	Henggou-2	Well	668	35	6.8	7100	− 81	− 10.8	< 1.0	− 6.0	5.4	1930
IS13	Stagnant area	May 2011	Henggou-1	Well	673	33	6.9	8930	− 83	− 11.1	< 1.0	− 5.3	5.8	2020

Note: /, not detected.
[a]Total dissolved solids.
[b]d-excess = δD-8xδ^{18}O.
[c]Recharge area altitude is calculated by δ^{18}O.

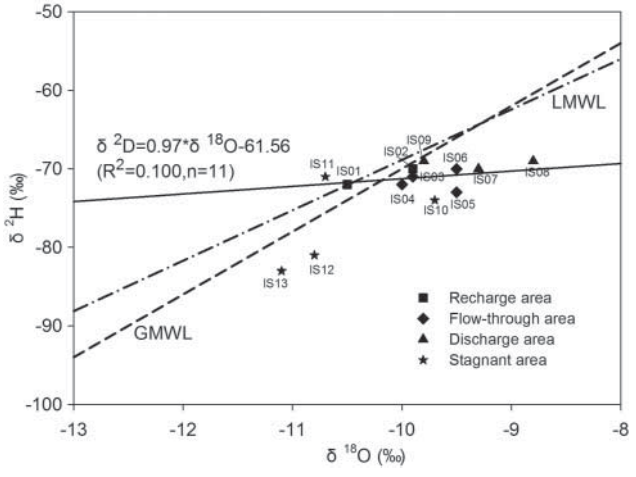

Figure 4. Relations between δ^2H and δ^{18}O values in the Liulin spring area. The solid line represents the regression line of groundwater samples.

Compared to the GMWL ($\delta^2H = 8 \times \delta^{18}O + 10$), the lower slope of the LMWL is attributed to non-equilibrium fractionation caused by evaporation during the dropping of the rainfall through a relatively dry air column. The more intensive the evaporation effect is, the lower the slope will be [1], especially for small rainfall events. The δ^2H values of the karst groundwater range from -83 to -69 ‰ with a mean value of -73 ‰, while the δ^{18}O values range between -11.1 and -8.8‰ with a mean value of -10.0 ‰. The values of these two isotopes in groundwater are lower than those in precipitation, which may be caused by the higher recharge altitude of groundwater than the elevation of the Taiyuan Station.

The mean δ^2H values of the groundwater in the recharge area, flow-through area and spring discharge area are -71, -71.5 and -69.5‰, respectively, while the mean δ^{18}O values are -10.2, -9.8 and -9.3 ‰, respectively. The values of δ^2H are almost identical after considering the analytical uncertainty (± 2 ‰), while the δ^{18}O values show an increasing trend along the groundwater flow path. The variations in the δ^2H and δ^{18}O values may be caused by the various altitudes of the recharge area and recharge source (such as surface water or precipitation). The mean d-excess values have a decreasing trend from recharge area to discharge area with values of 10.6, 5.6 and 5.4 ‰, respectively. The mean values of δ^2H and δ^{18}O decrease to -77 ‰ and -10.4 ‰ in the stagnant area, while the mean value of d-excess rises to 7.4 ‰. This suggests that the karst groundwater may come from a higher recharge altitude or form under cold climate conditions [1].

The relationship between δ^2H and δ^{18}O values of water samples is shown in Figure 4. Generally speaking, these samples plot mostly below, but not far from, the LMWL and GMWL with two exceptions (IS01 and IS11), indicating that precipitation is the primary recharge source of karst groundwater. Samples IS01–IS04 are close to the LMWL and GMWL, while IS05–IS13 show a certain offset from LMWL and GMWL. This indicates that δ^2H and δ^{18}O values may be affected by some other factors during runoff processes, such as mixing with groundwater from a relatively lower altitude area or leakage of the Sanchuan river.

The slope of the regression line (fitting by samples IS01 $\sim$ IS11) is lower than that of the LMWL and GMWL, indicating that evaporation effect occurs during rainfall infiltration into thicker unsaturated zones in the recharge area [1,35]. Furthermore, mixing with surface water is not ignorable.

It should be noted that the δ^2H and δ^{18}O values of IS12 and IS13, located in the stagnant area, show a large offset from the LMWL and GMWL and even from the other samples, which suggests that recharge and runoff conditions in the stagnant area are different from that in other regions. Moreover, mean temperature and total dissolved solids (TDS) of IS12 and IS13 reach up to 34 °C and 8015 mg/L, far higher than those of samples IS01–IS11, which shows the long-term water–rock interactions. Considering that water–rock reaction has no effect on δ^2H and δ^{18}O values at low temperature (< 90 °C) [36], we speculate that the groundwater with significantly depleted δ^2H and δ^{18}O values is recharged in a cold period (such as the last glacial period).

4.1.2. *Altitude of recharge region*

The values of δ^2H and δ^{18}O in precipitation decrease with the increase in altitude, known as the altitude effect. This effect, which could be conserved during recharge and flow-through processes, could be used to calculate the altitude of the recharge region of groundwater and surface water by using Equation (3) [1,2,9,23,34,36–38]. δ^{18}O values show an apparent negative correlation with the altitude of the sampling sites, especially in the upgradient of the Liulin spring where the Pearson correlation coefficient (R) reaches up to -0.731. It is important to note that the calculated attitude for a given sample denotes the mean altitude of its recharge region as groundwater usually represents a mixed signal recharged from various elevations [2].

$$H = \frac{\delta_S - \delta_P}{K} + h, \tag{3}$$

where H is the altitude of the recharge region; δ_S and δ_P denote the δ^{18}O values in samples and precipitation, respectively, in Taiyuan Station and δ_P is -7.24 ‰ here; K represents the altitude gradient of the δ^{18}O value (-0.31 ‰/100 m) [38] and h is the altitude of the meteorological station. The calculated recharge elevations rounded to 10 m are shown in Table 1.

The calculated altitude of Wucheng sample (IS01), pertaining to a relatively independent hydrogeological unit in the study area, is 1830 m asl, equivalent to the altitude of the exposed region of carbonate rocks in this unit ($\sim$ 750 to 1850 m asl). The calculated recharge altitudes of the samples in recharge area, the flow-through area, the discharge area and the stagnant area are 1640, 1510–1670, 1280–1600 and 1570–2020 m, respectively, consistent with the elevation of the recharge area. Considering the altitude of the recharge area near the Liulin spring ($\sim$1000 m asl) and in the south-east region ($\sim$1500–2100 m asl), the Liulin springs, with a mean recharge altitude of 1440 m asl, could be regarded as the mixture of groundwater recharged from the nearby and south-east regions.

4.2. *Runoff features of karst groundwater flow*

4.2.1. *Characteristics of ^{3}H contents*

Tritium (^{3}H) has a half-life of 12.43 yr (years). For spontaneous radioactive decay and insusceptibility to the water–rock interaction, ^{3}H, in the form of HTO in the hydrological cycle, is considered an ideal tracer to trace groundwater flow [1].

The higher the ^{3}H contents in groundwater are, the better the runoff conditions in the aquifer would be, and vice versa. If ^{3}H is detectable in one sample, the groundwater belongs to recent water recharged in the last 50 years, and must actively take part in the hydrological cycle. In general, the ^{3}H contents in the samples vary from 26.7 $\pm$ 1.9 TU in Wucheng to less than 1 TU (i.e. the detection limit) in Henggou with a mean value of 8.62 $\pm$ 1.72 TU, showing a slightly decreasing trend along the flow path. In the recharge area, the ^{3}H content in groundwater, falling

between 20.8 and 26.7 TU, is close to that in precipitation (about 27 TU) [27,28], indicating good flow conditions and a frequent exchange rate among precipitation, surface water and groundwater. In the stagnant area, the ^{3}H contents decrease quickly, and are even less than the detection limit near the west boundary. The ^{3}H contents of spring samples range from 7.1 to 9.0 TU with a mean value of 8.2 TU, and are higher than that in some of the upgradient samples in the flow-through area, such as the IS03 and IS04. This phenomenon may be caused by mixing between nearby and long-distance recharged groundwater [28]. This mixing effect mainly takes place in the region adjacent to the Liulin spring, and the travel time between the mixing region and discharge is finite. Mixing ratios for various end-members could be approximately calculated using the isotopic mass balance equation [36]. Assuming that the concentration and amount of a certain isotope in groundwater are C and N, respectively, we obtain

$$C_a N_a + C_b N_b = CN, \tag{4}$$

and

$$N_a + N_b = N, \tag{5}$$

where C_a, N_a and C_b, N_b represent values of concentration and amount of a and b end-member, respectively; N_a/N_b is the mixing ratio. Substituting Equation (5) into Equation (4), we obtain the following equation:

$$\frac{N_a}{N_b} = \frac{C_a - C}{C - C_b}. \tag{6}$$

For ^{3}H, we obtain

$$P_{a/b} = \frac{{}^3H_b - {}^3H_m}{{}^3H_m - {}^3H_a}, \tag{7}$$

where $P_{a/b}$ is the mixing ratio of a and b end-members; ^3H_b, ^3H_a and ^3H_m are the ^{3}H contents of precipitation groundwater with long flow path (the mean value of IS04 and IS05, i.e. 3.7 TU), and spring samples (a mean value of 8.2 TU). Substituting the aforementioned values in Equation (4), we obtain a value of 4.18 for $P_{a/b}$. Thus, the mixing ratio of karst groundwater with long flow path and short flow path in spring water is approximately 4:1. It must be emphasised that the calculated ratio is just an approximate value for neglecting the impact of travel time on ^{3}H contents.

4.2.2. *Characteristics of ^{13}C contents*

The ^{13}C isotope can be a good tracer of open and closed system evolution of DIC in groundwater [1]. The value of δ^{13}C is mainly dominated by dissolution of soil CO_2 and carbonate minerals. For large differences in δ^{13}C between the soil CO_2 and carbonate minerals, we are allowed to qualitatively evaluate the main source of HCO_3^- using Equations (8)–(11). Considering that HCO_3^- is the primary component of DIC as the pH value ranges from 6.8 to 7.9, the value of $\delta^{13}C_{HCO3}$ in samples is approximated by $\delta^{13}C_{DIC}$ (i.e. the measured values in Table 1).

$$CO_2 + H_2O \Leftrightarrow H_2CO_3 \tag{8}$$

$$H_2CO_3 \Leftrightarrow HCO_3^- + H^+ \tag{9}$$

$$CaCO_3 + H^+ \Leftrightarrow Ca^{2+} + HCO_3^- \tag{10}$$

$$CaMg(CO_3)_2 + 2H^+ \Leftrightarrow Ca^{2+} + Mg^{2+} + 2HCO_3^- \tag{11}$$

The δ^{13}C value of soil CO_2 is in the order of -25 ± 1 ‰ due to the prevalence of C_3 plants in the study area [39]. Carbon isotope fractionation only correlates with water temperature and

could be calculated according to Mook et al. [40].

$$\varepsilon_{g/b} = \delta_g - \delta_b = \frac{-9483}{T} + 23.89‰, \tag{12}$$

or Vogel et al. [41]

$$\varepsilon_{a/g} = \delta_a - \delta_g = \frac{-373}{T} + 0.19‰. \tag{13}$$

From (12) and (13), we obtain:

$$\varepsilon_{a/b} = \delta_a - \delta_b = \frac{-9866}{T} + 24.12‰. \tag{14}$$

Rubinson and Clayton [42] and Emirch et al. [43] give

$$\varepsilon_{s/b} = \delta_s - \delta_b = \frac{-4232}{T} + 15.10‰, \tag{15}$$

where ε = fractionation, g = gaseous CO_2, a = dissolved CO_2, b = dissolved HCO_3^-, s = solid calcite and $T = t\,°C + 273.15$ K.

When water temperature is close to 12 °C (IS02), $\varepsilon_{a/g} = \delta_a – \delta_g = -1.12$ ‰, $\varepsilon_{a/b1} = \delta_a – \delta_{b1} = -10.48$ ‰ and $\varepsilon_{s/b2} = \delta_s – \delta_{b2} = 0.25$ ‰. Here, δ_{b1} denotes the $\delta^{13}C$ value of HCO_3^- stemming from soil CO_2, and δ_{b2} is the $\delta^{13}C$ value of HCO_3^- from carbonate rocks. Assuming $\delta_g = -25$ ‰ (soil CO_2) and $\delta_s = 0$ (marine carbonate rocks), we can obtain $\delta_{b1} = -15.64$ ‰, $\delta_{b2} = -0.25$ ‰. Thus, the variation in $\delta^{13}C$ value for HCO_3^- ($\delta^{13}C_{HCO3}$) could be due to the mixing of two recharge sources as stated earlier.

The $\delta^{13}C_{HCO3}$ value of the karst groundwater could be considered as the mean value of δ_{b1} and δ_{b2} (-7.70 ‰) when the mixing ratio of the HCO_3^- from soil CO_2 and marine carbonate rocks is ~1:1. When the $\delta^{13}C_{HCO3}$ value of the HCO_3^- is less than -7.70‰, the dissolution of soil CO_2 can be regarded as a major source for HCO_3^-. If this value is greater than -7.70‰, the HCO_3^- is mainly derived from the dissolution of carbonate rocks. In the upgradient of the Liulin spring, almost all $\delta^{13}C_{HCO3}$ values are less than -7.70‰, which suggests that the HCO_3^- is mainly from the dissolution of soil CO_2. In the downgradient of the Liulin spring, these values are greater than -7.70‰, indicating that the HCO_3^- is mainly from the dissolution of carbonate rocks.

4.2.3. *Residence time of karst groundwater*

The ^{14}C isotope is used to calculate the groundwater ages of DIC worldwide [44]. The radiocarbon age (for Libby half-life, 5570 yr) in years BP (i.e. before 1950 AD) is calculated by [2,45]

$$t = 19035 \lg\left(\frac{A_0}{A_s}\right), \tag{16}$$

where t is the ^{14}C age of DIC in karst groundwater; A_0 and A_s denote the initial activity (100 pMC) and measured activity in water samples, respectively. The ^{14}C age of DIC calculated using Equation (16) (also called apparent ^{14}C ages) needs to be revised because A_0 could be diluted by the superimposed influence of hydrochemical reactions, physical processes and geohydraulic

Table 2. Calculated and corrected ^{14}C ages of karst groundwater.

No.	Sampling sites	$A^{14}C$ (pMC)	Results	
			Apparent ^{14}C ages of DIC (k yr)	Corrected ^{14}C ages of DIC (yr)
IS01	Wucheng	74.44 ± 1.27	2.44 ± 0.14	Modern
IS02	Youfangping	88.86 ± 1.99	0.98 ± 0.19	Modern
IS03	Tianjiahui	65.38 ± 1.32	3.51 ± 0.17	Modern
IS04	Shang'an	49.44 ± 1.36	5.82 ± 0.23	Modern
IS05	Jinluo	51.31 ± 1.14	5.52 ± 0.19	Modern
IS07	Shangqinglong	53.70 ± 1.20	5.10 ± 0.20	Modern
IS08	Yangjiagang	52.80 ± 1.40	5.30 ± 0.30	Modern
IS10	Baijiayan	26.80 ± 1.00	10.90 ± 0.30	2440
IS12	Henggou 2#	10.10 ± 0.70	19.00 ± 0.60	7155
IS13	Henggou 1#	9.60 ± 0.80	19.40 ± 0.70	6549

Note: pMC, % modern carbon; DIC, dissolved inorganic carbon.

mixing [46]. Thus, Equation (16) is transformed into [2]

$$t = 19035 \lg\left(F \times \frac{A_0}{A_s}\right), \tag{17}$$

where F denotes the correction coefficient (also called the dilution factor) and depends on the ^{14}C correction model applied. The karst groundwater system could be regarded as a closed system with respect to soil CO_2 due to the large depth of the groundwater level (more than 100 m in most of the study area). Therefore, the Pearson model [47] may be employed to calculate F value neglecting isotopic fractionation upon precipitation and dissolution of carbonate [48]

$$F = \frac{\delta^{13}C_{DIC}}{-25}, \tag{18}$$

where $\delta^{13}C_{DIC}$ denotes the $\delta^{13}C$ values of DIC in groundwater. The calculated results are shown in Table 2. More commonly, the Pearson model can highly overestimate groundwater age, but is still an improvement over uncorrected ages [1].

The apparent ^{14}C age of DIC in groundwater increases from 0.98 ± 0.19 k yr in the recharge area to 19.40 ± 0.70 k yr in the stagnant area. After revision by the Pearson model, samples located in the upgradient of the Liulin spring (including the Liulin spring) represent the modern groundwater features, indicating a positive flow condition. The detectable tritium contents in IS01–IS09 also reflect the modern groundwater features. The ^{14}C age of DIC shows a remarkable increase in the downgradient of the Liulin spring and reaches ∼7 k yr in Henggou, indicating a poor flow condition. The mean flow rate resulting from ^{14}C ages of DIC between IS10 and IS12 (about 5.8 km) is 1.23 m/year. The depleted δ^2H and $\delta^{18}O$ values in the stagnant area could also reflect the characteristics of old groundwater.

5. Conclusions

The use of environmental isotope techniques in studying the Liulin spring area has provided valuable information about the characteristics of this karst groundwater flow system. The major conclusions of this study are as follows:

(1) The groundwater mainly originates from precipitation. Remarkable evaporation occurs during dropping and infiltration of rainfall, and results in a certain offset of groundwater

samples from GMWL and LMWL. The karst groundwater, showing remarkably depleted δ^2H and δ^{18}O values in the stagnant area, may be recharged in a cold period.

(2) The mean recharged elevation of groundwater samples, ranging from 1280 to 2020 m asl, is consistent with the altitude of the recharge area. The calculated recharged altitude for the Liulin spring indicates a mixing between nearby and long-distance groundwater.

(3) The ^{3}H contents of groundwater show a generally decreasing trend along the flow path and are used to calculate the mixing effect occurring in spring waters. The mixing ratio between nearby and long-distance recharge groundwater is 1:4.

(4) In the upgradient of the Liulin spring, HCO_3^- of groundwater is mainly derived from the dissolution of soil CO_2, while that in the downgradient of the Liulin spring is derived from the dissolution of carbonate rocks.

(5) The samples located in the upgradient of the Liulin spring show modern groundwater features. The ^{14}C age of DIC increases remarkably in the downgradient of the Liulin spring with a mean flow rate of 1.23 m/year between IS10 and IS12.

Acknowledgements

The authors would like to thank Guoqing Wang, Shuyan Xing and Fei Zhang for their help on hydrochemical and isotopic sampling campaigns, data collections and technical support.

Funding

This research was financially supported by the International S&T Cooperation Program of China [grant number 2012DFA20770] and Shanxi Provincial Natural Science Foundation [grant number 2010011030-1]. The work was also supported by Lvliang Municipal Water Management Committee Office, Lvliang, China.

References

[1] Clark I, Fritz P. Environmental isotopes in hydrology. Boca Raton, FL: Lewis Publishers; 1997.

[2] Wang H. 同位素水文地质学概论 [Introduction to isotopic hydrogeology]. Beijing: Geology Publishing House; 1991.

[3] Gu W, Pang Z, Wang Q, Song X, Ye N, Zhang Z, Lu J, Lu B, Qu S. 同位素水文学 [Isotope hydrology]. Beijing: Science Press; 2011.

[4] Marfia AM, Krishnamurthy RV, Atekwana EA, Panton WF. Isotopic and geochemical evolution of ground and surface waters in a karst dominated geological setting: a case study from Belize, Central America. Appl Geochem. 2004;19:937–946.

[5] Gammons CH, Brown A, Poulson SR, Henderson TH. Using stable isotopes (S, O) of sulfate to track local contamination of the Madison karst aquifer, Montana, from abandoned coal mine drainage. Appl Geochem. 2013;31:228–238.

[6] Cartwright I, Weaver TR, Cendón DI, Fifield LK, Tweed SO, Petrides B, Swane I. Constraining groundwater flow, residence times, inter-aquifer mixing, and aquifer properties using environmental isotopes in the southeast Murray Basin, Australia. Appl Geochem. 2012;27:1698–1709.

[7] Carucci V, Petitta M, Aravena R. Interaction between shallow and deep aquifers in the Tivoli Plain (Central Italy) enhanced by groundwater extraction: a multi-isotope approach and geochemical modeling. Appl Geochem. 2012;27:266–280.

[8] Chelnokov G, Kharitonova N, Bragin I, Vasileva M. Deuterium, oxygen-18 and tritium in precipitation, surface and groundwater in the Far East of Russia. Procedia Earth Planet Sci. 2013;7:151–154.

[9] Ettayfi N, Bouchaou L, Michelot J, Tagma T, Warner N, Boutaleb S, Massault M, Lgourna Z, Vengosh A. Geochemical and isotopic (oxygen, hydrogen, carbon, strontium) constraints for the origin, salinity, and residence time of groundwater from a carbonate aquifer in the Western Anti-Atlas Mountains, Morocco. J Hydrol. 2012;438–439:97–111.

[10] Falcone RA, Falgiani A, Parisse B, Petitta M, Spizzico M, Tallini M. Chemical and isotopic (oxygen-18, deuterium, carbon-13, radon-222) multi-tracing for groundwater conceptual model of carbonate aquifer (Gran Sasso INFN underground laboratory–central Italy). J Hydrol. 2008;357:368–388.

[11] Kendall C, Coplen TB. Distribution of oxygen-18 and deuterium in river waters across the United States. Hydrol Processes. 2001;15:1363–1393.

[12] Marques JM, Graça H, Eggenkamp HG, Neves O, Carreira PM, Matias MJ, Mayer B, Nunes D, Trancoso VN. Isotopic and hydrochemical data as indicators of recharge areas, flow paths and water–rock interaction in the Caldas da Rainha–Quinta das Janelas thermomineral carbonate rock aquifer (Central Portugal). J Hydrol. 2013;476:302–313.
[13] Sappa G, Barbieri M, Ergul S, Ferranti F. Hydrogeological conceptual model of groundwater from carbonate aquifers using environmental isotopes (oxygen-18, deuterium) and chemical tracers: a case study in southern Latium Region, central Italy. J Water Resour Prot. 2012;4:695–716.
[14] Pu T, He Y, Zhang T, Wu J, Zhu G, Chang L. Isotopic and geochemical evolution of ground and river waters in a karst dominated geological setting: a case study from Lijiang basin, South-Asia monsoon region. Appl Geochem. 2013;33:199–212.
[15] Prtoljan B, Kapelj S, Dukarić F, Vlahović I, Mrinjek E. Hydrogeochemical and isotopic evidences for definition of tectonically controlled catchment areas of the Konavle area springs (SE Dalmatia, Croatia). J Geochem Explor. 2012;112:285–296.
[16] Yoshimura K, Nakao S, Noto M, Inokura Y, Urata K, Chen M, Lin P. Geochemical and stable isotope studies on natural water in the Taroko Gorge karst area, Taiwan – chemical weathering of carbonate rocks by deep source CO_2 and sulfuric acid. Chem Geol. 2001;177:415–430.
[17] Li X, Liu C, Harue M, Li S, Liu X. The use of environmental isotopic (C, Sr, S) and hydrochemical tracers to characterize anthropogenic effects on karst groundwater quality: A case study of the Shuicheng Basin, SW China. Appl Geochem. 2010;25:1924–1936.
[18] Lee ES, Krothe NC. A four-component mixing model for water in a karst terrain in south-central Indiana, USA. Using solute concentration and stable isotopes as tracers. Chem Geol. 2001;179:129–143.
[19] Koh YK, Choi BY, Yun S, Choi HS, Mayer B, Ryoo SW. Origin and evolution of two contrasting thermal groundwaters (CO_2-rich and alkaline) in the Jungwon area, South Korea: Hydrochemical and isotopic evidence. J Volcanol Geoth Res. 2008;178:777–786.
[20] Gonfiantini R, Zuppi GM. Carbon isotope exchange rate of DIC in karst groundwater. Chem Geol. 2003;197:319–336.
[21] Fonyuy EW, Atekwana EA. Dissolved inorganic carbon evolution and stable carbon isotope fractionation in acid mine drainage contaminated streams: insights from a laboratory study. Appl Geochem. 2008;23:2634–2648.
[22] Craig H. The geochemistry of the stable carbon isotopes. Geochim Cosmochim Acta. 1953;3:53–92.
[23] Kattan Z. Environmental isotope study of the major karst springs in Damascus limestone aquifer systems: case of the Figeh and Barada springs. J Hydrol. 1997;193:161–182.
[24] Yang Y, Shen Z, Weng D, Hou G, Zhao Z, Wang D, Pang Z. Oxygen and hydrogen isotopes of waters in the Ordos Basin, China: implications for recharge of groundwater in the north of Cretaceous Groundwater Basin. Acta Geol Sin. 2009;83:103–113.
[25] Lin L, Wang J. [Analysis of isotope and water chemistry in karst groundwater in Shanxi-Shaanxi george]. Geotech Invest Surv. 2004:27–29. Chinese.
[26] Ma T, Wang Y, Guo Q, Yan C, Ma R, Huang Z. Hydrochemical and isotopic evidence of origin of thermal karst water at Taiyuan, northern China. J Earth Sci. 2009;20:879–889.
[27] Hou G, Zhang M, Liu F, Wang Y, Liang Y. 鄂尔多斯盆地地下水勘查研究 [Groundwater exploration in the Ordos basin]. Beijing: Geology Publishing House; 2008.
[28] Groundwater exploration project in the Ordos basin (China). Karst groundwater expliotation of Liulin-Wubu district in Shanxi and Shaanxi province. Taiyuan: Geological survey institute of Shanxi province (China); 2004.
[29] Gran G. Determination of the equivalence point in potentiometric titrations. Analyst. 1952;77:661–671.
[30] Brand WA, Coplen BT, Vogl J, Rosner M, Prohaska T. Assessment of international reference materials for isotope-ratio analysis (IUPAC Technical Report). Pure Appl Chem. 2014;86:425–467.
[31] Coplen TB. Guidelines and recommended terms for expression of stable-isotope-ratio and gas-ratio measurement results. Rapid Commun Mass Spectrom. 2011;25:2538–2560.
[32] The GNIP database: Global Network of Isotopes in Precipitation [Internet]. Vienna: International atomic energy agency (IAEA)/World Meteorological Organization (WMO). [cited 1986～1988]. Available from: http://www.iaea.org/water
[33] Craig H. Isotopic variations in meteoric waters. Science. 1961;133:1702–1703.
[34] Zheng S, Hou F, Ni B. [Study on stable hydrogen and oxygen isotopes in precipitation in China]. Chin Sci Bull. 1983;28:801–806. Chinese.
[35] Pienitz R, Douglas MSV, Soml JP. Long-term environmental change in Aritic and Antarctic lakes. Dordrecht: Kluwer Academic Publishers; 2003.
[36] Mook WG. Environmental isotopes in the hydrological cycle. Paris: United Nations Educational, Scientific and Cultural Organization; 2000.
[37] Van Geldern R, Kuhlemann J, Schiebel R, Taubald H, Barth JAC. Stable water isotope patterns in climate change hotspot: the isotope hydrology framework of Corsica (western Mediterranean). Isot Environ Health Stud. 2014;50:184–200.
[38] Huang P, Chen J, Ning C. [The analysis of hydrogen and oxygen isotopes in the groundwater of Jiaozuo mine area]. J Chin Coal Soc. 2012;37:770–774. Chinese.
[39] Amundson R, Stern L, Baisden T, Wang Y. The isotopic composition of soil and soil-respired CO_2. Geoderma. 1998;82:83–114.

[40] Mook WG, Bommerson JC, Staverman WH. Carbon isotope fractionation between dissolved bicarbonate and gaseous carbon dioxide. Earth Planet Sci Lett. 1974;22:168–175.
[41] Vogel JC, Grootes PM, Mook WG. Isotope fractionation between gaseous and dissolved carbon dioxide. Z Phys. 1970;230:225–238.
[42] Rubinson M, Clayton RN. Carbon-13 fractionation between aragonite and calcite. Geochim Cosmochim Acta. 1969;33:997–1002.
[43] Emrich K, Ehhait D, Vogel JC. Carbon isotope fractionation during the precipitation of calcuim carbonate. Earth Planet Sci Lett. 1970;8:363–371.
[44] Libby WF, Johnson F. Radiocarbon dating. Chicago: University of Chicago Press; 1955.
[45] Stenström KE, Skog G, Georgiadou E, Genberg J, Johansson A. A guide to radiocarbon units and calculations. Lund: Lund University, Department of Physics, Division of Nuclear Physics; 2011.
[46] Mebus AG. An overview of carbon-14 analysis in the study of groundwater. Radiocarbon. 2000;42:99–114.
[47] Pearson FJ, Noronha CJ, Andrews RW. Mathematical modeling of the distribution of natural carbon-14, uranium-234, and uranium-238 in regional groundwater system. Radiocarbon. 1983;25:291–300.
[48] Buckau G, Artinger R, Kim JI, Geyer S, Fritz P, Wolf M, Frenzel B. Development of climatic and vegetation conditions and the geochemical and isotopic composition in the Franconian Albvorland aquifer system. Appl Geochem. 2000;15:1191–1201.